Mechanical Systems and Signal Processing 139 (2020) 106645

Contents lists available at ScienceDirect

Mechanical Systems and Signal Processing

journal homepage: www.elsevier.com/locate/ymssp

Multiple leak detection algorithm for pipe network

Sang Hyun Kim

Department of Environmental Engineering, Pusan National University, San 30 Jangjundong Kumjunggu, Pusan 609-735, Republic of Korea

ARTICLE INFO

Article history:
Received 16 March 2019
Received in revised form 31 October 2019
Accepted 12 January 2020
Available online 23 January 2020

Keywords:
Pipeline system
Multiple leak detection
Sequential leak detection algorithm
Single path algorithm
Dual path algorithm

ABSTRACT

In this work, several important issues and solutions are considered in order to develop a method for multiple leak detection in pipe network systems. To relax the model complexity and ameliorate parsimony problems, a mathematical formulation of the occurrence of multiple leaks in a pipe network is proposed, which also provides flexibility for multiple leak representation. To identify the leakage signal from the complex pressure variation of a pipe network, a decomposition scheme to obtain a pressure signal from a transient wave according to its interaction with multiple leaks is developed. Considering the wave transmission characteristics of a disturbed pressure wave obtained for a leak in a pipeline element by a pressure sensor, a sequential leak detection algorithm (composed of single and dual path algorithms) for application to the identified leakage signal is developed. While the single path algorithm uses the principle of time domain reflectometry, the dual path algorithm extends the pressure responses to address multiple pressure pathways. A multiple leak detection example for a heterogeneous pipe network demonstrates the potential of the developed methods and, also, addresses the nonlinear interaction between multiple leaks and the pipe network structure.

1. Introduction

Leakage detection in pipeline systems is an important avenue of engineering research, not only to facilitate proper water-loss management, but also to maintain reliable drinking water quality and prevent pathogen intrusion into distribution systems [1–3]. Based on inverse transient analysis [4], pressure wave reflection for an abnormal boundary condition has been widely used for leak detection in pipeline systems [5–17]. In most leak detection studies, the pressure wave is generated by maneuvering the control valve attached to the water distribution system. The transient pressure wave can be generated through manual opening of the valve [18] (or opening of a solenoid valve) of a portable pressure tank to generate discrete pressure signals [19], or even by using an electrical spark generator to create sharp pressure pulses [20]. The transient-based method for pipeline abnormality detection can also be applied to discrete blockages [21,22], dead-end side branches [15,23], and pipe wall deterioration [24]. Analysis of abnormal pressure waves can be conducted either in the time [24,25] or frequency [6,7,10,11,16,26–28] domains, or both [14].

However, although most existing leak detection approaches focus on detection of a single leak, leakage problems in real-world pipeline systems frequently arise as multiple leaks. Multiple leak detection has been explored in the frequency domain through analytical formulations for pressure responses [10]. In particular, knowledge of the leakage response pattern is important for design of an efficient formulation for multiple leak representation; for example, such a formulation has previously been implemented in a multiple leak detection algorithm for a simple reservoir pipeline valve system [29].

E-mail address: kimsangh@pusan.ac.kr

https://doi.org/10.1016/j.ymssp.2020.106645
0888-3270/

Maximum likelihood estimation has also been used to identify leak locations and sizes in the case of multiple leaks; however, the interactions between the leaks were neglected in those studies [30,31]. Existing studies for multiple leaks have been performed under single pipeline examples and a further elaboration is required for the leak detection of complicate pipe network systems.

1.1. Problem statement

Detection of multiple leaks in a pipe network can be an extremely challenging problem for several reasons, one of which is the transient signal complexity. The many pathways, loops, and branches of the pressure waves in pipe networks complicate the pressure signal, which is undesirable for leak detection. Another factor is the number of unknown parameters. If this number exceeds six (i.e., there are three leaks), multiple local optima issues can affect the widely used metaheuristic calibration engines. Another important aspect is that the problem dimension for the multiple leak case cannot be known a priori in field systems [31]. An unknown number of leaks requires a robust leak detection algorithm, which must be adaptive and capable of acquiring the number of unknown parameters through signal analysis [29].

An additional challenging issue concerns the mathematical representation of multiple leaks in a pipe network. The mathematical formulation complexity tends to increase significantly with the number of leaks, and its implementation in the corresponding model for proper representation of the pipe network system and in the leakage prediction procedure become difficult.

Unlike the relatively simple, straight, and visually identified pattern of a single-leak response of a simple pipeline system [18,32], the pressure response pattern in a pipe network is complex and almost indeterminable through visual inspection. The pressure reflection from a leak propagates into the network structure and the leakage response circulates among loops and bounces between branches, generating a pressure response that is difficult to analyze. The pressure pulse generated from a valve maneuver and its interaction with the pipeline components of a pipe network are merged with the complex pressure reflections from the leak. Identification of the solitary leakage response from the pressure signal can become increasingly difficult as the numbers of pipeline elements, loops, and branches are increased.

If multiple leaks exist in a pipe network system, the interaction between each leakage response and the remaining pipe structure can be even more complex than in the case of a single leak. Thus, it is extremely difficult to identify the impact and impulse pressure response caused by the valve action for multiple leaks, and also to determine the interference of a specific leak effect among the total leak responses [30]. The detectability of a specific leak can vary with increasing leaks, because the resonance pattern of multiple leaks with the loops and branches can vary under different leakage conditions.

The wave propagation pattern from a leak in a looped section must also be considered. A looped pipeline section can be distinctly characterized based on the leakage information transferred to the pressure sensor. This is because the transient signal for a specific leak can be delivered in multiple directions and its reflection also follows multiple pathways. Proper consideration of wave travel paths is very important for appropriate design of an efficient multiple leak detection algorithm.

1.2. Objectives

The ability to distinguish the response patterns of different components (e.g., particular leak and pipe network structures) from among the total pressure response is an important requirement for multiple leak detection in pipe network systems. Fundamental understanding of complex pressure response patterns is a critical component of an effective leak detection scheme, because the multiple paths of the pressure signal to the pressure sensor can introduce considerable difficulty as regards multiple leak calibration of pipe network systems.

Therefore, three objectives are accomplished in this study, which can constitute important building blocks for efficient multiple leak detection schemes for pipe network systems:

- First, an efficient multiple leak formulation (MLF) is developed for computation and calibration of multiple leaks in pipe network systems;
- Second, a decomposition method for leakage signal identification from the transient pressure response of a pipe network system is proposed.
- Third, a sequential leak detection scheme involving a single path algorithm, a dual path algorithm, and holistic calibration, are developed considering the wave propagation characteristics towards the pressure sensor and the effects of leakage interference.

To demonstrate the potential of the developed techniques as regards realization of an efficient multiple leak detection algorithm, a hypothetical pipe network system is considered and the proposed methods are implemented.

2. Methods

2.1. Transient responses in pipe network with multiple leaks

Unsteady flow in a pipeline can be described by the following momentum and continuity equations [33,34]:

$$\frac{\partial Q}{\partial t}+gA\frac{\partial H}{\partial x}+\frac{f|Q|Q}{2DA}=0 \tag{1}$$

$$\frac{\partial H}{\partial t}+\frac{a^2}{gA}\frac{\partial Q}{\partial x}=0 \tag{2}$$

where x is the distance along the pipe, t is time, a is the wave speed, g represents the gravitational acceleration, A is the pipe cross sectional area, Q is the discharge of flow, H is the head, f is the Darcy-Weisbach friction factor, and D is the pipe diameter.

Assuming a steady oscillatory flow with linearized friction, the relationships between an upstream and a downstream head-discharge point as a function of x can be expressed in the complex domain as follows [33]:

$$H(x)=H_U cosh\gamma x-Z_C Q_U sinh\gamma x \tag{3}$$

$$Q(x)=-H_U/Z_C sinh\gamma x+Q_U cosh\gamma x \tag{4}$$

where subscript U denotes an upstream section; the propagation constant, $\gamma=\sqrt{Cs'(Ls'+R)}$; the characteristic impedance, $Z_C=\gamma/Cs'$; the complex frequency can be defined as s' σ= +iω; the capacitance, $C = gA/a^2$; the inertance, $L = 1/gA$; the resistance, $R=32\nu/gAD$ or $f\overline{Q}/gA^2D$, depending upon whether laminar or turbulent flow is present; and σ and ω represent a decay factor and frequency, respectively.

The hydraulic impedance, $H(X)/Q(x)$, at a certain point can be derived through application of Eqs. (3) and (4) to all elements of a pipe network, for a common head condition at a joint point in the pipe network:

$$H_{a1}=H_{a2}=\cdots=H_{an} \tag{5}$$

where H_{a1} and H_{a2} are the heads at junction node a for pipe sections 1 and 2, respectively, and n is the number of elements joined to the junction.

Continuity equations for a junction are necessary to define the mass balance with consideration of the flow direction. Here,

$$\sum_{i=1}^{n}Q_{ai}=0 \tag{6}$$

where Q_{ai} is the complex discharge at junction node a for pipe element i.

Eqs. (3)–(6) can be manipulated to obtain an expression for the reference discharge, Q_r, so as to obtain a generalized impedance formulation. In detail, application of the impedance formation from Eqs. (3) and (4) to all pipe elements, implementation of the common hydraulic impedance formation from Eq. (5), and use of the continuity of the discharge ratio from Eq. (6) into all junctions provides the following impedance matrix equations [35]:

$$\begin{bmatrix} Z_C sinh\gamma_i l_i & 1 & 0 & \cdots & & & \cdots \\ -cosh\gamma_i l_i & 0 & 1 & \cdots & & & \cdots \\ 0 & 0 & 1 & \cdots & & & \cdots \\ 0 & -cosh\gamma_j l_j & 0 & Z_C sinh\gamma_j l_j & 1 & 0 & \cdots \\ \cdot & sinh\gamma_i l_i/Z_C & 0 & -cosh\gamma_j l_j & 0 & 1 & \cdots \\ \cdot & \cdot & \cdot & \cdot & \cdot & \cdot & \cdots \\ & \cdots & & \cdots & & & \cdots \\ & \cdots & & \cdots -cosh\gamma_x l_x & \cdot & 1 & 0 \\ & \cdots & & \cdots sinh\gamma_x l_x/Z_C & \cdot & 0 & 1 \end{bmatrix} \cdot \begin{bmatrix} H_i/Q_r \\ Q_i/Q_r \\ Q_r/Q_r \\ H_j/Q_r \\ Q_j/Q_r \\ \cdot \\ \cdot \\ H_x/Q_r \\ Q_{zk}/Q_r \end{bmatrix} = \begin{bmatrix} 0 \\ 0 \\ 1 \\ 0 \\ 0 \\ \cdot \\ \cdot \\ 0 \\ 0 \end{bmatrix} \tag{7}$$

where subscript zk represent downstream valve. The matrix formulation for multiple leaks (m) in the complex domain for a given element can be derived from Eqs. (3) and (4) as follows [6]:

$$\begin{bmatrix} H_D/Q_r \\ Q_D/Q_r \end{bmatrix} = \begin{bmatrix} cosh\gamma y_{m+1} & -Z_C sinh\gamma y_{m+1} \\ -sinh\gamma y_{m+1}/Z_C & cosh\gamma y_{m+1} \end{bmatrix} \cdot \begin{bmatrix} 1 & 0 \\ Q_{olk,m}/2H_o & 1 \end{bmatrix} \cdots\cdots \begin{bmatrix} 1 & 0 \\ Q_{olk,1}/2H_o & 1 \end{bmatrix} \cdot \begin{bmatrix} cosh\gamma y_1 & -Z_C sinhy_1 \\ -sinh\gamma y_1/Z_C & cosh\gamma y_1 \end{bmatrix} \cdot \begin{bmatrix} H_U/Q_r \\ Q_U/Q_r \end{bmatrix} \tag{8}$$

where H_U/Q_r, H_D/Q_r, Q_U/Q_r, and Q_D/Q_r are impedances and complex head ratios of the upstream and downstream boundaries of a pipeline element, respectively; $Q_{olk,i}$ is the mean discharge of the ith leak; H_o is the mean head pressure; and $y_{m+1},\cdots y_1$ are the distances between the leaks and the boundary of the pipeline element.

Considering the structure of the impedance matrix shown in Eq. (7) and rearranging Eq. (8), the impact of multiple leaks can be incorporated into the impedance matrix structure as follows:

$$\begin{bmatrix} 1 & 0 & Z_{ii} & Z_{ij} \\ 0 & 1 & Z_{ji} & Z_{jj} \end{bmatrix} \cdot \begin{bmatrix} H_i/Q_r \\ Q_i/Q_r \\ H_j/Q_r \\ Q_j/Q_r \end{bmatrix} = \begin{bmatrix} 0 \\ 0 \\ 0 \\ 0 \end{bmatrix} \tag{9}$$

where $Z_{ii}, Z_{ij}, Z_{ji}, Z_{jj} = f(\gamma, x_1, \cdots x_{m+1}, Q_{olk,1}, \cdots, Q_{olk,m}, H_o, Z_C)$. Substitution of Eq. (9) into Eq. (7) provides the impedance matrix for a pipe network with multiple leaks. Furthermore, application of the modified lower–upper (LU) decomposition scheme from [33] to the complex linear system provides the solution vector. The ratios of an arbitrary pressure head to a specific discharge impulse or an arbitrary discharge to a specific discharge can be obtained from division of the solution vectors obtained from Eq. (7).

The pressure response function in the time domain, $r_{hx}(t)$, can be obtained through application of a Fourier transform to the ratio function from the solution vector, as follows:

$$r_{hx}(t) = \frac{1}{\pi} \cdot Re\left[\int_0^\infty (\frac{H_x}{Q_{zk}}) e^{i\omega t} d\omega\right] \tag{10}$$

where *Re* denotes the "real part of." and subscript x represent any designated point. In addition, the discharge response function for any designated point x for a discharge impulse in the time domain, $r_{qx}(t)$, can be expressed as follows:

$$r_{qx}(t) = \frac{1}{\pi} \cdot Re\left[\int_0^\infty \left(\frac{Q_x}{Q_{zk}}\right) e^{i\omega t} d\omega\right] \tag{11}$$

The time series of the pressure head or discharge at a point can be obtained through convolution of the discharge impulse at the downstream valve in the pipe network.

2.2. Efficient multiple leak function for impedance matrix

The number of terms and complexity of Eqs. (8) and (9) can increase considerably with the number of leaks, which can yield an extremely complex impedance matrix. In a previous study, a multiple leak function was developed for a simple reservoir pipeline valve system in terms of the hydraulic impedance, with implementation of unsteady friction models for laminar and turbulent flows [29]. A similar approximation for multiple leaks has also been presented in linear matrix form for behavior under steady friction [30]. However, development of a generalized MLF for a pipe network is required for efficient expression of such behavior and for incorporation in impedance matrixes such as those of Eqs. (7) and (9). The complex head-discharge and discharge-discharge ratio relationships for a single leak pipeline element between upstream and downstream can be expressed as follows, through application of the hyperbolic trigonometric function addition formulas:

$$\frac{H_D}{Q_r} = \left(cosh\gamma l + Z_c \frac{Q_{olk}}{2H_o} sinh\gamma(l-x) cosh\gamma x\right) \frac{H_U}{Q_r}$$

$$-Z_c(sinh\gamma l + Z_c \frac{Q_{olk}}{2H_o} sinh\gamma(l-x) sinh\gamma x) \frac{Q_U}{Q_r} \tag{12}$$

$$\frac{Q_D}{Q_r} = -\left(\frac{sinh\gamma l}{Z_c} + \frac{Q_{olk}}{2H_o} cosh\gamma(l-x) cosh\gamma x\right) \frac{H_U}{Q_r} + (cosh\gamma l + Z_c \frac{Q_{olk}}{2H_o} cosh\gamma(l-x) sinh\gamma x) \frac{Q_U}{Q_r} \tag{13}$$

where x is the distance to the leak from the downstream point.

Introduction of multiple leaks into Eqs. (12) and (13) and sequential applications of the hyperbolic function addition formulas provide the following algebraic expressions for the effects of multiple leaks:

$$\frac{H_D}{Q_r} = \left(cosh\gamma l \frac{H_U}{Q_r} - Z_c sinh\gamma l \frac{Q_U}{Q_r}\right) + (Z_c \sum_{i=1}^{m} \frac{Q_{olk,i}}{2H_o} sinh\gamma(l-x_i) cosh\gamma x_i) \frac{H_U}{Q_r} - (Z_c{}^2 \sum_{i=1}^{m} \frac{Q_{olk,i}}{2H_o} sinh\gamma(l-x_i) sinh\gamma x_i) \frac{Q_U}{Q_r}$$
$$+ \sum_{n=2}^{m} [\prod_{j=1}^{n} \left(\frac{Q_{olk,k}}{2H_0}\right)_{(k=C(m,n))} \{f_1(Z_c, sinh\gamma y_l, cosh\gamma y_l)_{l=1,n+1} \frac{H_U}{Q_r} + f_2(Z_c, sinh\gamma y_l, cosh\gamma y_l)_{l=1,n+1} \frac{Q_U}{Q_r}\}] \tag{14}$$

$$\frac{Q_D}{Q_r} = -\frac{sinh\gamma l}{Z_c} \frac{H_U}{Q_r} + cosh\gamma l \frac{Q_U}{Q_r} - \sum_{i=1}^{m} \frac{Q_{olk,i}}{2H_o} cosh\gamma(l-x_i) cosh\gamma x_i \frac{H_U}{Q_r} + Z_c \sum_{i=1}^{m} \frac{Q_{olk,i}}{2H_o} cosh\gamma(l-x_i) sinh\gamma x_i)$$
$$\frac{Q_U}{Q_r} \sum_{n=2}^{m} [\prod_{j=1}^{n} \left(\frac{Q_{olk,k}}{2H_0}\right)_{(k=C(m,n))} \{f_3(Z_c, sinh\gamma y_l, cosh\gamma y_l)_{l=1,n+1} \frac{H_U}{Q_r} + f_4(Z_c, sinh\gamma y_l, cosh\gamma y_l)_{l=1,n+1} \frac{Q_U}{Q_r}\}] \tag{15}$$

where $C(m,n)$ is the combination of m taking n and f_1, f_2, f_3 and, f_4 are hydraulic impedance functions and hyperbolic trigonometric functions between leaks and boundaries.

The terms having $\prod_{j=1}^{n}\left(\frac{Q_{olk,k}}{2H_0}\right)_{(k=C(m,n))}$ in Eqs. (14) and (15) are negligible because of the small amplitude (of the order of −3 to −6) of $\frac{Q_{olk,k}}{2H_0}$. Further, double or more than triple multiplications of this term can be even smaller. Eqs. (14) and (15) can be feasibly incorporated into the impedance matrix. Indeed, incorporation of these efficient multiple leak expressions into the impedance matrix with unsteady friction is shown in Appendices A and B, for laminar and turbulent flow conditions, respectively.

2.3. Leakage signal decomposition

Detection of multiple leaks from pressure signals in a pipe network is a challenging problem, because the pressure pulse is affected not only by the pressure wave interaction with the pipeline components (such as loops), the features of the pipeline elements (e.g., the length, diameter, and elastic property), and the topological structure of the pipe network, but also by the interaction between the multiple leak signal with various features of the pipe network. Therefore, separation of the leakage impact from the combined pressure signal is very important for feasible analysis of multiple leaks in a pipe network.

Multiple leaks as hydraulic impedance can be identified in the frequency domain as follows:

$$\left(\frac{H_x}{Q_{zk}}\right)_{idenleak} = \frac{\left(\frac{H_x}{Q_r}\right)_{wleak}}{\left(\frac{Q_{zk}}{Q_r}\right)_{wleak}} - \frac{\left(\frac{H_x}{Q_r}\right)_{woleak}}{\left(\frac{Q_{zk}}{Q_r}\right)_{woleak}} \tag{18}$$

where $\left(\frac{H_x}{Q_r}\right)_{wleak}$, $\left(\frac{Q_{zk}}{Q_r}\right)_{wleak}$, $\left(\frac{H_x}{Q_r}\right)_{woleak}$, $\left(\frac{Q_{zk}}{Q_r}\right)_{woleak}$ are ratios of the complex head to reference discharge and the complex discharge to reference discharge with and without multiple leaks, respectively, which can be computed from the solutions of impedance matrix equations similar to Eq. (7). In this study, subscripts zk and x are the node 9 (the downstream valve) shown in Fig. 2. Solutions of impedance matrix having multiple leakages or without leakage resulted into either $\left(\frac{H_x}{Q_r}\right)_{wleak}$, $\left(\frac{Q_{zk}}{Q_r}\right)_{wleak}$ or $\left(\frac{H_x}{Q_r}\right)_{woleak}$, $\left(\frac{Q_{zk}}{Q_r}\right)_{woleak}$, respectively.

Simultaneous detection of multiple leaks can be very difficult, partially because of the many unknown parameters (e.g., if the number of leaks > 3), and also because the number of leaks is unknown in real-world systems. Therefore, separation of the signal for a particular leak from a multiple leak signal is an another important problem that must be overcome for design of an efficient multiple leak detection scheme for pipe network systems. The pressure signal of one leak in a pipe network (in the case of a single leak only) can differ from the signal for the same leak obtained from a multiple leak signal, because there can be interactions between distinct leakage signals and the pipe network structure. The signal for a particular leak j can be identified as hydraulic impedance from a multiple leak signal in the frequency domain as follows:

$$\left(\frac{H_x}{Q_{zk}}\right)_{leakj} = \frac{\left(\frac{H_x}{Q_r}\right)_{wleak}}{\left(\frac{Q_{zk}}{Q_r}\right)_{wleak}} - \frac{\left(\frac{H_x}{Q_r}\right)_{leakw/oj}}{\left(\frac{Q_{zk}}{Q_r}\right)_{leakw/oj}} \tag{19}$$

where $\left(\frac{H_x}{Q_r}\right)_{leakw/oj}$ and $\left(\frac{Q_{zk}}{Q_r}\right)_{leakw/oj}$ are ratios of the complex head to reference discharge and the complex discharge to reference discharge for multiple leaks without j, respectively.

The pressure head signal in the time domain for multiple leaks and for j from the multiple leak signal can be obtained through substitution of Eqs. (18) and (19) into Eq. (10).

2.4. Leakage element identification

Identification of a suspicious leakage element is an important pre-process for successful multiple leak detection in a pipe network. The pressure wave generated by the valve can be transmitted through multiple pathways to a designated leak point, and the reflected wave(s) can be transmitted back through multiple pathways. In other words, multiple pressure waves are delivered to a leak point and a bounced wave or waves can be multiplied back to the pressure sensor through multiple pathways. The forward pressure pathway with the shortest length (between the leak and valve) and the reflected pressure wave along the corresponding pathway constitute the first pressure response of the leakage. This information can be useful to identify the location of a specific leak.

The pressure wave can pass through the leak; the shifting information from the leak to the normal pipeline is then added into the passing pressure wave. As the passing wave reaches another node (either upstream or downstream), other multiple pathways to the pressure sensor can be established, which deliver conjugate pressure waves related to the leak. The reflected wave from a leak reduces the pressure response, but the wave passing through a leak creates a compensated pressure wave. Therefore, the pressure signal response at the sensor indicates the distance to a specific leak based on the round travel time along the shortest pathway, and also identifies a specific leakage element according to the time when the accumulated impact of the pressure reflections begins to be counteracted by conjugate pressure waves.

2.4.1. Pipeline element characterization

Depending on the pressure wave propagation features, the pipeline elements for a pipe network system can be divided into two categories: looped and non-looped. A looped pipeline element is part of a looped pipeline structure. The disturbance signal from the leak propagates and circulates in both clockwise and counterclockwise directions in this element. As the transient pressure signal approaches a specific leak from either the clockwise or counterclockwise direction, reflected and passing waves can be generated in counter and identical directions to the approaching wave, respectively. These two distinct wave transmissions introduce substantial complexity to the pressure wave responses of the pressure sensor. In a non-looped element, the propagation pattern of the abnormality information is similar to that of a simple reservoir pipeline valve system. Even though the interaction of the pressure signals between the looped and non-looped pipeline elements generates an even more complex pressure response, leak detection analysis can be easier for a non-looped than a looped pipeline element because of the feasibility of leak signal identification.

The wave propagation pattern in the looped pipeline element can be characterized into two different sections in the context of leakage detection: single and dual path. In the single path section, the frontal pattern of the pressure wave reflection for a leak is similar to that of a simple reservoir system. The arrival time of the beginning of the reflected wave indicates the shortest path length between the pressure sensor and a specific leak. In the dual path section in a looped pipe element, there are two different wave reflection pathways (clockwise and counterclockwise) for a leak, with the travel times to the pressure sensor being identical for both. Fig. 1 illustrates the single path section and the dual path section in a pipeline element located at the end of a looped pipeline system.

Therefore, application of a leak detection scheme using the principle of time domain reflectometry is undesirable for a dual path section. In other words, it is necessary to consider the extended pressure signal containing the wave pathway information of multiple connecting elements in order to detect a leak in a dual path section.

2.4.1.1. Leak detection algorithm for single path section. The leak detection algorithm for the single path section of a looped pipeline element, namely, the "single path algorithm," is identical to the leak detection algorithm for a non-looped pipeline element in a pipe network system. The single path algorithm procedure is as follows.

Step 1. The identified multiple leak pressure signal can be evaluated using Eqs. (7) to (18) or a modification of Eq. (18) using in-situ observations of a pressure signal for a pipe network system.

Step 2. The pressure gradient amplitudes can be calculated between i, the time step starting from 2, and t_s, the time step of the travel time to the end of the single path section, as follows:

$$|Grad| = \left| \frac{(h/H_0)_i - (h/H_0)_{i-1}}{t_i - t_{i-1}} \right| \tag{20}$$

where $(h/H_0)_i$ is the normalized identified leakage pressure by the steady pressure. If $|Grad|$ is greater than a designated minimum threshold (T_{min}), a frontal leakage signal can be assumed to be detected. Then, two dummy variables, $K1 = i - 3$ and $K2 = i - 1$, can be determined for the leakage location calibration ranges.

The minimum and maximum thresholds of the range for the travel time to a leak within the leakage element can be evaluated as follows:

$$T1 = K1 \cdot \Delta t - 2\sum_{j=1}^{nc} \frac{l_j}{a_j} \tag{21}$$

$$T2 = K2 \cdot \Delta t - 2\sum_{j=1}^{nc} \frac{l_j}{a_j} \tag{22}$$

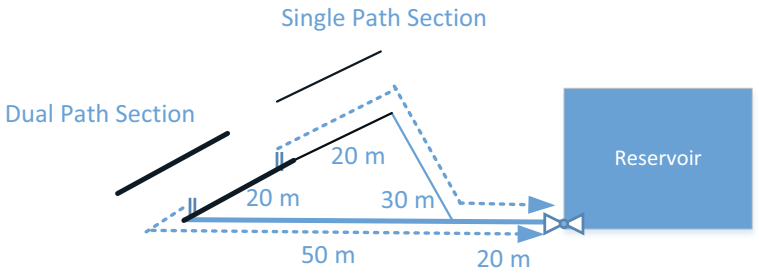

Fig. 1. Schematic of the single path section and the dual path section in a looped pipeline element. The dotted arrows represent dual pathways having an identical travel time to downstream valve from two different leakages.

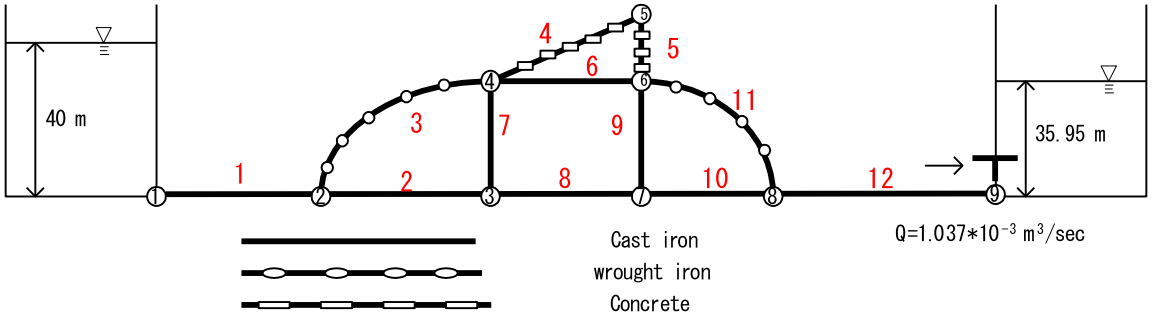

Fig. 2. Schematic of hypothetical pipe network system.

where *nc* is the number of connected elements in the shortest path between the pressure sensor and leakage element, l_j are the lengths of the connected pipeline elements, and a_j are the wave speeds of the connected pipeline elements. Therefore, the maximum and minimum leak location search thresholds in the leakage element, x_{min} and x_{max}, are

$$x_{min} = T1 \cdot a_k \cdot l_k/2 \tag{23}$$

$$x_{max} = T2 \cdot a_k \cdot l_k/2 \tag{24}$$

where l_k and a_k are the leakage element length and wave speed, respectively. The maximum and minimum search thresholds for the leak quantities can be defined as the percentages relative to the steady discharge of the leakage element, $q_{leak,min}$ and $q_{leak,max}$, respectively.

Step 3. The leak location and quantity, x_{leak} and q_{leak}, respectively, can be calibrated for ranges (x_{min}, x_{max}) and ($q_{leakmin}$, $q_{leakmax}$) using a metaheuristic engine (e.g., the genetic algorithm (GA) and particle swarm optimization (PSO)) [36,37]. The objective function for the single path algorithm (OFSPA) can be expressed as

$$\text{OFSPA} = \text{Minimize} \sum_{i1=K2}^{K2+is} \left[\left(\frac{h}{H_0}\right)_{i1,cal} - \left(\frac{h}{H_0}\right)_{i1,iden} \right]^2 \tag{25}$$

where *is* is a small time-step number that does not interfere with a possible adjacent leak, $\left(\frac{h}{H_0}\right)_{i1,cal}$ is the pressure signal obtained with calibrated x_{leak} and q_{leak}, and $\left(\frac{h}{H_0}\right)_{i1,iden}$ is the identified leakage signal.

Step 4. The optimum x_{leak} and q_{leak} are obtained from Step 3. Then, the optimized pressure head signal, $\left(\frac{h}{H_0}\right)_{i,opt}$, can be obtained. The identified pressure head signal should be revised as follows:

$$\left(\frac{h}{H_0}\right)_{i2,iden} = \sum_{i2=1}^{t_f} \left(\frac{h}{H_0}\right)_{i2,iden} - \left(\frac{h}{H_0}\right)_{i2,opt} \tag{26}$$

where t_f is the final time step for revising the pressure signal.

Step 5. To detect all leaks within the single path section, the procedure from Steps 2 to 4 is iterated until the time *i* in Step 2 is equal to t_s.

Once Step 5 is completed, the identified pressure signal is filtered for possible multiple leak impact within the single path section.

2.4.1.2. Leak detection algorithm for dual path section. The leak detection algorithm for the dual path section of the leakage element, namely, the "dual path algorithm," can only be applied if the single path algorithm is used to pretreat the identified leakage pressure signal. The procedure of the dual path algorithm is as follows.

Step 1. The filtered (identified) leakage signal can be refined through simultaneous consideration of multiple leaks (their locations and quantities) obtained from the single path algorithm.
Step 2. A search can be conducted for possible leaks between t_d and t_f, the time steps of the starting point of the dual path section and of the first wave reflection from the other reservoir boundary condition, respectively. The pressure response calibration period should be bounded to the time of wave reflection from the other constant head reservoir. This is because the impact of unsteady friction, which can substantially compromise the leak detection potential because of

uncertainties regarding parameters and distinct flow regimes, can be neglected for the period of the first wave reflection to the other constant head reservoir.

Step 3. One (or additional) leak(s) can be assumed, with corresponding leak locations and quantities, in the dual path section. The minimum and maximum leak location search thresholds are the two boundaries of the dual path section. The leak quantity ranges can be similarly designated to those for the single path algorithm.

Step 4. One (or additional) leak location(s) and quantity(quantities), x_{leak} and q_{leak}, can be calibrated using a metaheuristic engine. The objective function for the dual path algorithm (OFDPA) can be expressed as

$$\text{OFDPA} = \text{Minimize} \sum_{i3=2}^{t_f} \left\lfloor \left(\frac{h}{H_0}\right)_{i3,filt} - \left(\frac{h}{H_0}\right)_{i3,cal} \right\rfloor^2 \tag{27}$$

where $\left(\frac{h}{H_0}\right)_{i3,filt}$ is the filtered leakage signal and $\left(\frac{h}{H_0}\right)_{i3,cal}$ is the calibrated pressure signal.

Step 5. If the final OFDPA is less than a predefined criterion (a much smaller number), which should be zero for perfect calibration, the algorithm proceeds to Step 6. Otherwise, it is assumed that one more leak exists within the dual path section and the algorithm returns to Step 3.

Step 6. The multiple leak detection results can be obtained using the whitened pressure time series.

Sequential application of the single and dual path algorithms completes the multiple leak detection for the suspicious leakage element. Depending on the deviation degree of the whitened leakage pressure signal from zero and the user-defined calibration accuracy, further heuristic calibration (e.g., by increasing the iteration number) can yield an improved solution.

3. Results and discussion

3.1. Results

In this study, a hypothetical heterogeneous pipe network system (Fig. 2) was used for application and demonstration of the leak detection potentials of the developed schemes [35]. The properties of the multi-looped pipe network system, such as the pipe lengths, diameters, friction factors, and pipe materials, are presented in Table 1. Depending upon the diameter, wall thickness, and elastic modulus of the pipeline material, the wave propagation speeds of the pipeline elements varied between 1247 and 1452 m/s. The pipeline system conveyed water from an upstream constant head reservoir (40 m) to another constant head reservoir (35.95 m). A waterhammer could be generated by instant closure of the control valve located at the end of the pipeline connected to the downstream reservoir. To analyze the unsteady flow in the pipe network, a 32×32 impedance matrix was formulated. The LU decomposition solver for a complex linear system was used to obtain 32 ratios of the complex heads or discharges to the complex discharge in the frequency domain. The solution of the impedance matrix of Eq. (7) and its convolution in Eq. (10) showed good agreement with results obtained using the method of characteristics [35].

The multiple leak impact can be represented in the matrix using either the conventional leakage representation (CLR) of Eq. (9) or the efficient multiple leak formulation (MLF) developed herein using Eqs. (16) and (17). To compare the computational performance of the CLR and MLF, multiple leaks (5 and 10) with a leak quantity of 3% relative to the steady flow were assumed in pipeline element 3 shown in Fig. 2. The leak locations were 4, 12, 20, 28, and 36 m from node 4 for the case of five leaks, with the additional leaks for the 10-leak case being located at 44, 52, 60, 68, and 76 m from node 4. Fig. 3(a) and (b)

Table 1
Dimensions of hypothetical pipe network system shown in Fig. 2.

Pip element.	up node	Down node	Pipe material	l (m)	D (mm)	E (N/m^2) *10^{11}	a (m/s)	F
1	1	2	Cast Iron	100	40	1.34	1431.13	0.04
2	2	3	Cast Iron	60	40	1.34	1431.13	0.04
3	2	4	Wrought Iron	80	32	1.8	1451.53	0.032
4	4	5	Concrete	60.4	25	0.015	1247.34	0.05
5	5	6	Concrete	25	25	0.015	1247.34	0.05
6	4	6	Cast Iron	55	40	1.34	1431.13	0.04
7	3	4	Cast Iron	40	40	1.34	1431.13	0.04
8	3	7	Cast Iron	55	40	1.34	1431.13	0.04
9	6	7	Cast Iron	40	40	1.34	1431.13	0.04
10	7	8	Cast Iron	50	40	1.34	1431.13	0.04
11	6	8	Wrought Iron	70	32	1.8	1451.53	0.032
12	8	9	Cast Iron	150	40	1.34	1431.13	0.04

l: length; D: diameter; E: elastic modulus; a: wave speed; f: Darcy–Weisbach friction factor

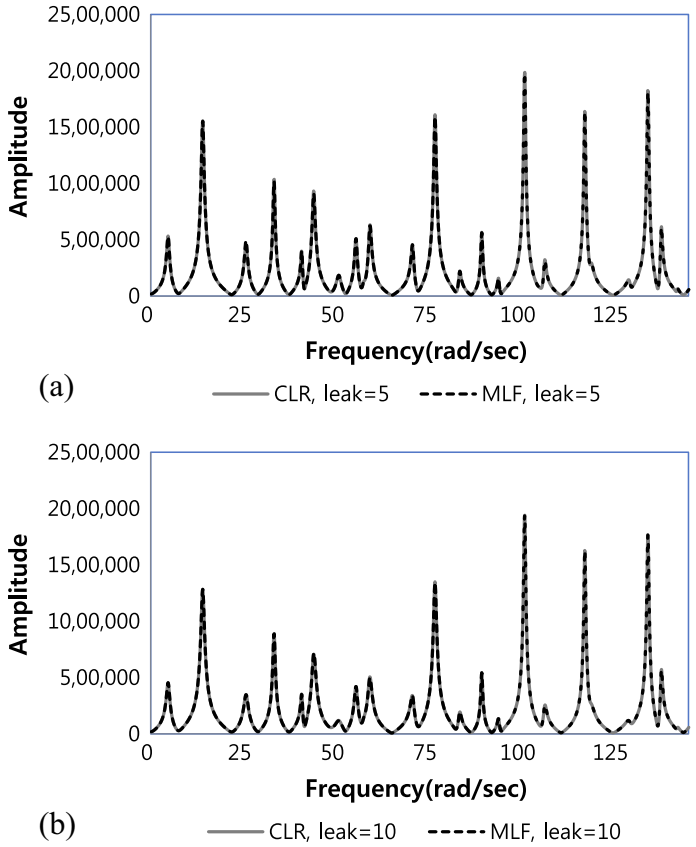

Fig. 3. Hydraulic Impedances (H/Q) at valve calculated using CLR and MLF under conditions of (a) 5 and (b) 10 leaks with leak quantity of 3% relative to steady flow rate, at pipeline element 3 of pipe network system.

present the hydraulic impedance (HI) at the control valve for 5 and 10 leaks, respectively, in pipeline element 3, with H_{zk}/Q_{zk} being calculated using the CLR and MLF. As apparent from Fig. 3, no difference in HI was found between the results obtained using the CLR and MLF.

However, the number of mathematical terms in the CLR and MLF vary significantly. Further, this difference increases considerably with the number of leaks. Fig. 4(a) shows the number of terms for CLR and MLF in accordance with the leak number for impedance matrix implementation in cases of steady and unsteady friction under laminar flow conditions (Appendix A). Those for unsteady friction and turbulent flow (Appendix B) are presented in Fig. 4(b). While the number of CLR terms for 10 leaks are 236,196 and 39,062,500 for laminar and turbulent flow with unsteady friction, respectively, those for MLF are 44 and 84, respectively. This indicates the outstanding parsimony of MLF for representation of multiple leaks in the impedance matrix formulation. Another strength of MLF over CLR is its flexibility in the order of multiple leakage considerations, which allow the implementation of the single path algorithm and the dual path algorithm in leakage detection schemes for looped elements of pipe network systems.

Assuming five leaks at locations 8, 24, 40, 56, and 72 m from node 4 at element 3 with a leak quantity of 7% relative to the steady flow rate, the HI at the control valve was calculated, along with the corresponding HI without leakage, as shown in Fig. 5(a). The similarity between the two HIs can be explained by the pipe network structure (e.g., by the connectivity between the pipeline elements, lengths, and wave speeds). The impact of the five leaks on the transient wave is responsible for substantial mitigation in the peak amplitudes for the corresponding HI compared to the leak-free HI. Fig. 5(b) presents the HI of the identified five leaks at element 3 obtained from Eq. (18), which addresses the interaction between the five leaks and the remaining pipeline structure of the system. Note that a somewhat similar HI to Fig. 5(b) can be obtained through subtraction of the leak-free HI from the five-leak HI. However, the difference between the HI for the identified leaks and the subtracted HI cannot be negligible in terms of accuracy (not shown here). This is because the round-off error of the hydraulic impedance can be substantial for computations for a complex pipe network.

Fig. 6(a) presents the normalized pressure responses at the control valve for the five-leak and leak-free conditions of Fig. 5(a). The pressure response under the five-leak condition exhibited more damped pressure fluctuations than those for the leak-free case. This is because the presence of leaks causes surge mitigation in both the time (Fig. 6(a)) and frequency domains (Fig. 5(a)). The pressure response for the identified leaks is shown in Fig. 6(b), which was obtained through

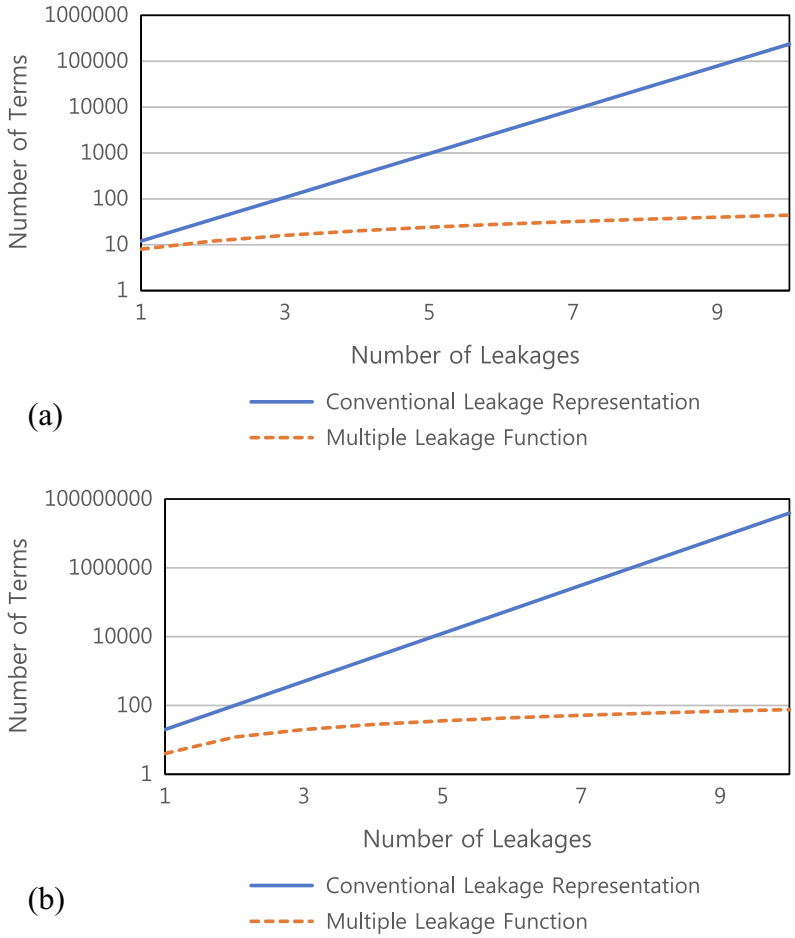

Fig. 4. Relationship between number of mathematical terms and number of leaks for CLR and MLF for (a) steady and unsteady friction with laminar flow and (b) unsteady friction with turbulent flow.

convolution of the HI shown in Fig. 5(b). This is the normalized impact of the five leaks in element 3 and their interactions with other parts of the pipeline structure, excluding the signal of the conventional waterhammer (e.g., the valve action and the wave reflection from other reservoirs). In other words, Fig. 6(b) provides a solitary basis for multiple leak detection without the impact of the transient generation and its decay process.

The other underlying interaction influencing the identified multiple leak pressure is the interference between the leakage and pipeline structure. The change in HI for different leak numbers indicates the contribution of a particular leak among all other leaks to the HI; however, this can be different to the HI of the particular leak itself. Here, an HI was calculated for leaks positioned at 8, 24, 56, and 72 m from node 4 at element 3, and then subtracted from the five-leak HI. A comparison between the HI of one leak at the 40-m location in element 3 and that corresponding to the subtraction of the abovementioned 4-leak HI from the 5-leak HI is shown in Fig. 7(a). The contribution of one leak out of five leaks (leak 3(diff.) in Fig. 7(a)) is apparently less than that of the same leak when it appears as a single leak only (leak 3 in Fig. 7(a)). This result indicates that detection of an particular leak (with a specific location and quantity) in a multiple leak situation can be more challenging than detection of the same leak under single-leak conditions. Therefore, the damping of a particular leak in the HI is greater in the case of multiple leaks and increases with the leak number. In fact, the difference between leak 3 and leak 3(diff.) in Fig. 7(a) indicates that the interaction impact of the pipeline structure in the case of multiple leaks is different to that of a particular leak at the 40-m location in element 3 in the frequency domain. The time domain responses (normalized pressures) for leak 3 and leak3(diff.) in Fig. 7(a) are shown in Fig. 7(b). The pressure response signal for leak 3 under five-leak conditions, i.e., leak 3 (diff.), shows more damped variation than that for a single leak (leak 3), which is consistent with the HI results.

Appropriate identification of a leakage-suspected element is an important requirement for the efficient multiple leak detection scheme. The identified leakage pressure response can be very useful for leakage element identification. For five leaks with 7% leak quantity distributed at 0.1, 0.3, 0.5, 0.7 and 0.9 length ratios for pipeline elements 9, 6, and 3, the identified leakage pressure signals are presented in Fig. 8. The start times of the significant pressure signals (the wave reflection from the leaks) for elements 9, 6, and 3 are 0.29, 0.32 and 0.40 s, respectively, which correspond exactly with the round travel time

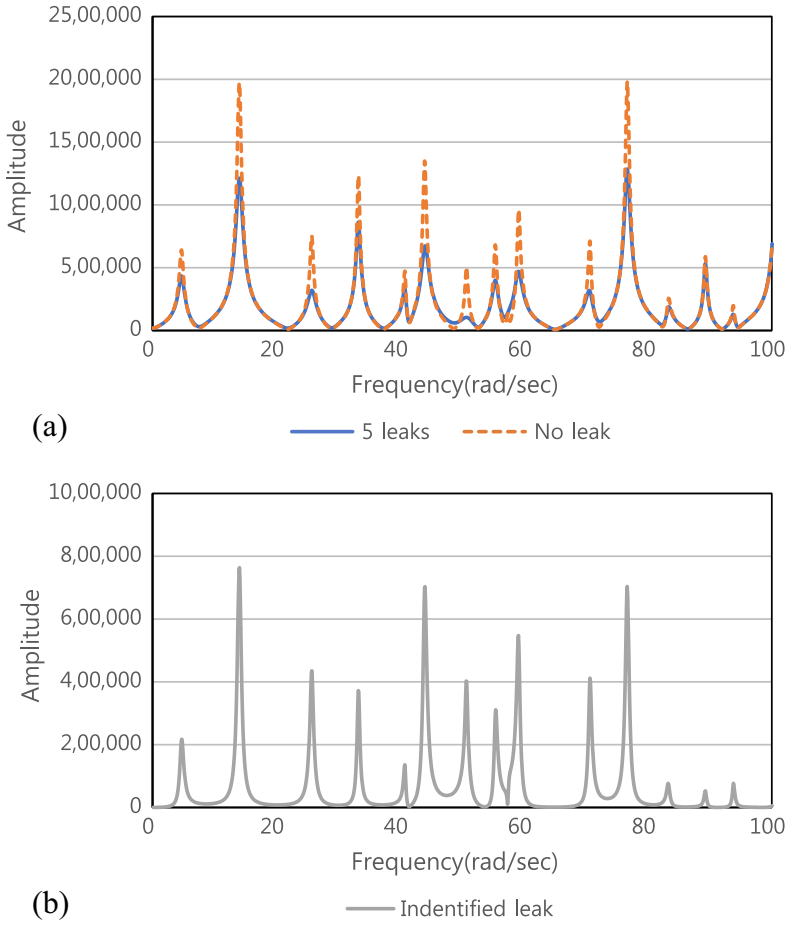

Fig. 5. (a) Hydraulic Impedances (H/Q) for five leaks at element 3 and for case without leakage. (b) H/Q of five identified leaks at element 3 at pipe-network control valve.

of the wave to the control valve for the first leak of each element. The first passing wave of the leaks arrived back at the valve after 0.32, 0.4, and 0.47 s for elements 9, 6, and 3, respectively. Negative reductions of the pressure waves were observed after the arrival times of the first passing waves for all three elements, which indicate that the multiple pathways for the waves passing over the leaks began to counteract the multiple pathways of the waves reflected from the leaks (Fig. 8). The signals for multiple leaks in other elements also showed distinct starting points and compensated pressure responses to each other. In order to confirm the identification potential of a leak-suspected element, the sum of the absolute identified pressure differences between all leakage element combinations were computed. The average and standard deviation of all pressure difference combinations per unit time step between 0 and 0.57 s (Fig. 8) were 0.054 and 0.027 h/H_0, respectively. These results indicate distinct features among the pressure differences, resulting from the different start times and inflection times of the pressure responses.

Assuming five leaks with 7% leak quantity located at 8, 24, 40, 56, and 72 m from node 4 in pipeline element 3, the identified leakage pressure signal was generated for multiple leak detection. Note that element 3 can be divided into two sections: a single path section between 0 and 41.56 m from node 4 and a dual path section between 41.56 and 80 m from node 4. The travel time of a wave from the valve to elements 12, 11, 6 and the 41.56 m point of element 3 is identical to the travel time from the valve to elements 12, 10, 8, and 2, being approximately 0.22 s. This means that a wave from a leak at 41.56 m from node 4 and a wave from a leak at an adjacent point of node 2 share a common arrival time at the valve. In fact, there are numerous dual points having identical travel times to the valve within the dual path section. Therefore, application of the single path algorithm is only valid for the single path section of element 3.

When the single path algorithm was applied to the identified multiple leak signal (labeled "5 leaks" in Fig. 9(a)), the leakage frontal signal could be detected from the time series of $|Grad|$. The optimization parameters were specified as T_{min} = 0.08 and is = 2, which depend on the computation time interval (Δt) and the background noise level for the pressure signal. The minimum and maximum leak quantity search thresholds were 0 and 20% of the steady flow rate, respectively. Once the optimum leak location and quantity were obtained, the identified multiple leak signal was revised by subtracting a single

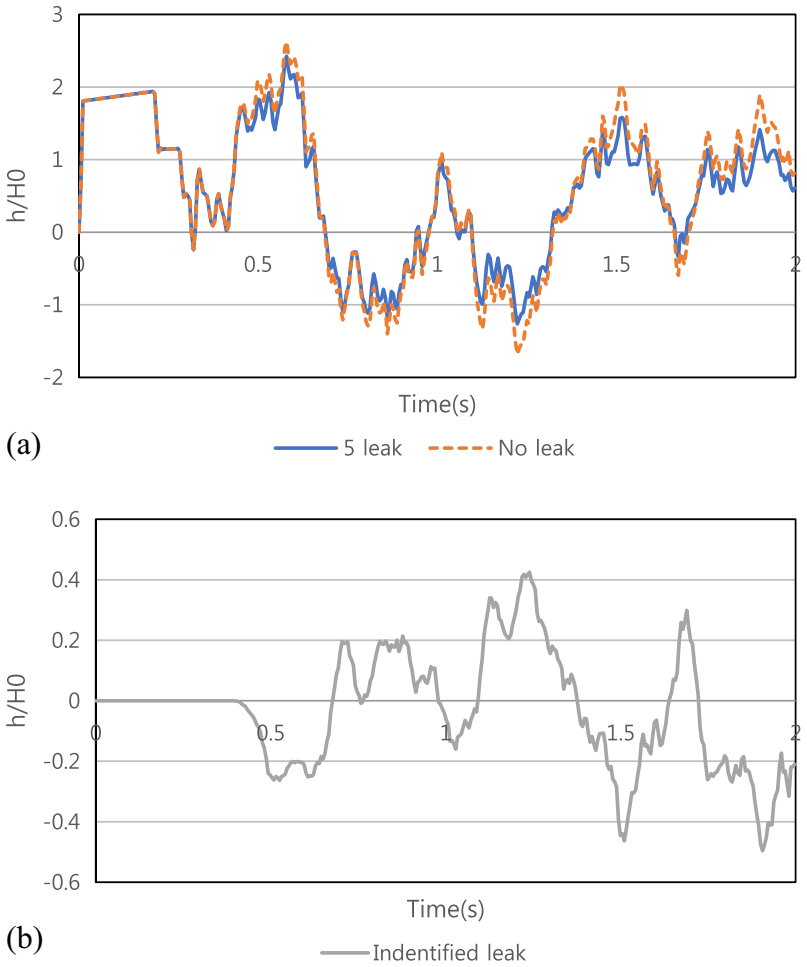

Fig. 6. Normalized pressure responses (a) for five leaks at element 3 and for case without leakage and (b) for five identified leaks at element 3 at pipe-network control valve.

leakage signal using the optimized leak location and quantity. The revised signals considering the first leak (denoted "filtered leak 1"), first and second leaks (denoted "filtered leak 1, 2"), and first, second, and third leaks (denoted "filtered leak 1, 2, 3") are shown in Fig. 9(a). Note that the interference between leaks did not affect the single path algorithm performance because the travel time of the first pressure wave reflection is not affected by the presence of the other leaks. In addition, the OFSPA in Eq. (23) requires very small time steps (is = 2) for calibration.

The final revised signal from the single path algorithm can be used for application of the dual path algorithm. When identical optimization parameters were submitted to the single path algorithm, a predefined criterion of 0.005 was used for the OFDPA to calibrate the leakage information for the dual path section. The final time step for calibration, t_f, was 0.58 s, which corresponds to the round travel time between the two reservoirs. Two iterations of the dual path algorithm satisfied the predefined OFDPA criterion. Fig. 9(b) presents the identified leakage signal, the optimized leakage signal, and the whitened signal. The whitened signal (Fig. 9(b)) exhibited deviation from 0.487 s, which indicates that the leakage prediction error is mainly associated with the dual path section. Table 2 presents the leak detection results of the single and dual path algorithms. The errors in the leak location predictions for the single path algorithm were 0.2, 0.7, and 0.2 m, but those for the dual path algorithm were 3.5 and 1.5 m. The errors in leak quantity for the single path algorithm were 0.1, 0.4, and 0.4% relative to the steady flow rate, but those for the dual path algorithm were 0.8 and 1.4%. The greater prediction error in the dual path section can be explained by the fact that the calibration error tends to accumulate and the leak prediction accuracy naturally decreases in later iterations of the sequential leak detection scheme. However, for the calibration for the dual path section, the simultaneous interference between the five leaks and pipeline structure was neglected. This is because the filtered signal individually removed the impact of each leak. When the three leaks determined by the single path algorithm were implemented as known leak information, one further calibration of two leaks for the dual path section was performed between the identified leakage signal and calibration signal. Table 3 presents the two leak predictions of the dual path section obtained from the simultaneous calibration. The accuracy of the two leak locations in Table 3 is better than those for

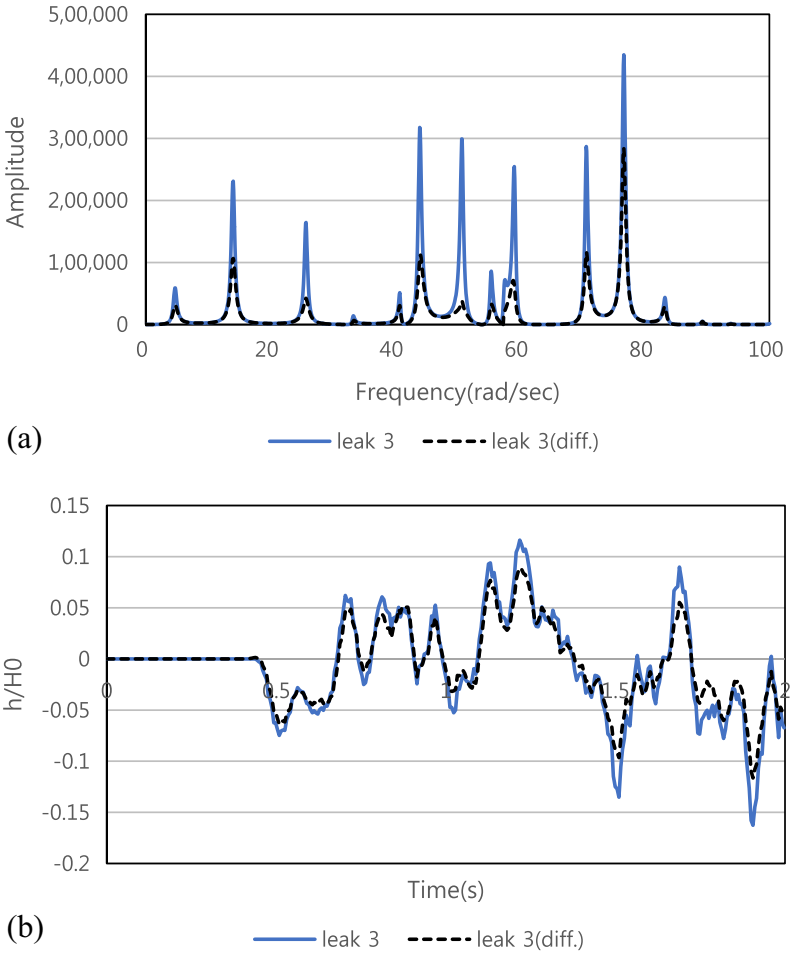

Fig. 7. (a) Hydraulic impedance of leak at 40 m in element 3 determined for five-leak condition (leak 3(diff.)) and that for single leak at 40 m in element 3 (leak 3). (b) Normalized pressure (time domain) responses of leak 3(diff.) and leak 3 at pipe-network valve.

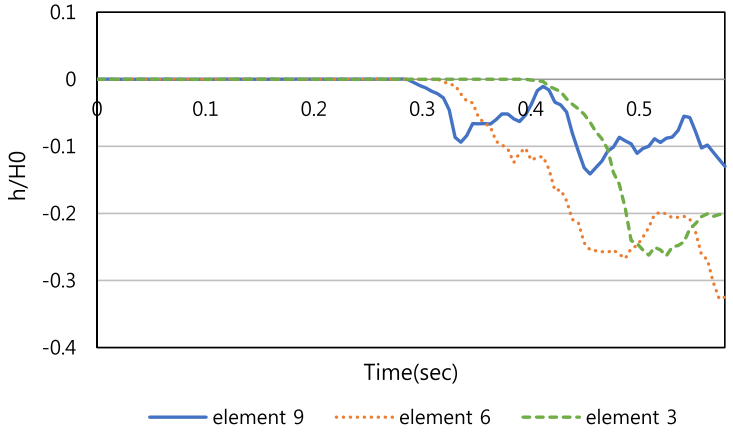

Fig. 8. Normalized identified leakage pressure responses under five-leak condition with leak quantity of 7% relative to steady flow rates for elements 9, 6, and 3.

Table 2; however, the leak quantity results seem to have similar accuracy as previously. This may partially be because of the accumulated error in predictions by the single path algorithm, and partially because the leak quantity has lower sensitivity than the leak location; thus, a minor calibration discrepancy tends to be expressed in terms of leak quantity uncertainty.

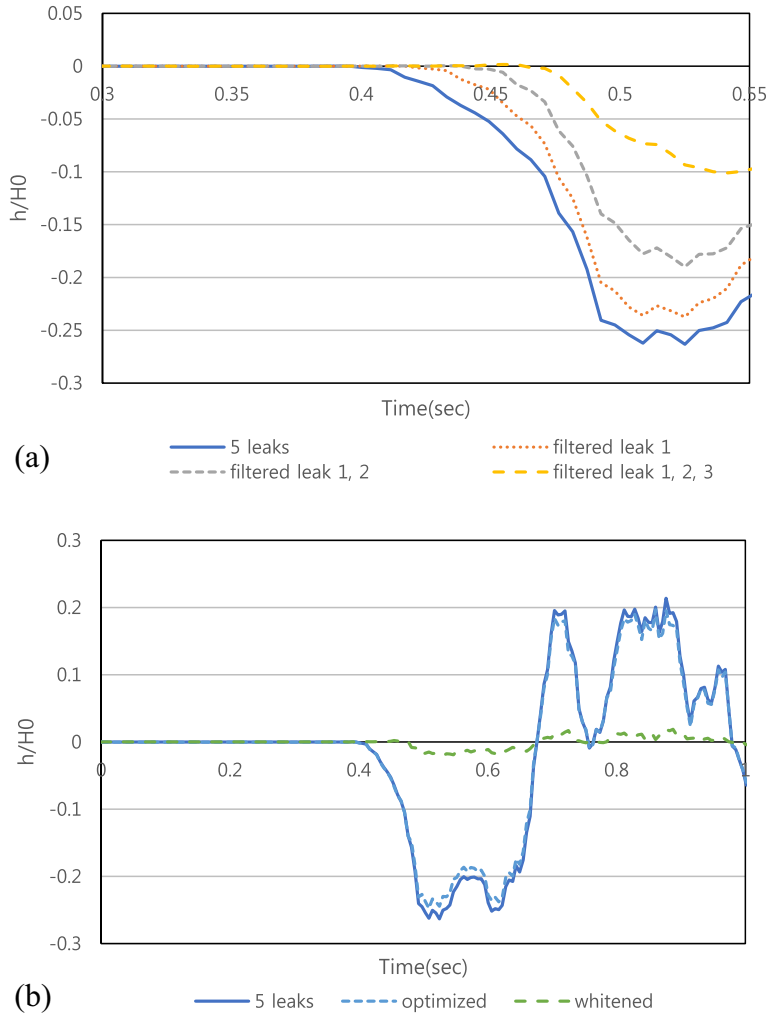

Fig. 9. (a) Normalized pressure signal for identified leakage (5 leaks) and pressure signals filtered by removal of 1st leak signal (filtered leak 1), 1st and 2nd leak signals (filtered leak 1, 2), and 1st, 2nd, and 3rd leak signals (filtered leak 1, 2, and 3). (b) Normalized pressure signal for identified leakage (5 leaks), optimized pressure signal (optimized), and whitened pressure signal (whitened).

Table 2
Leak detection results of single and dual path algorithms for five leaks in element 3 of pipe network.

Scheme	The single path algorithm	The dual path algorithm			
Leak location	7.8 m (8.0 m)	23.3 m (24.0 m)	38.8 m (40.0 m)	59.5 m (56.0 m)	73.5 m (72.0 m)
Leak quantity	6.9% (7.0%)	6.6% (7.0%)	7.4% (7.0%)	6.2% (7.0%)	5.6% (7.0%)

The numbers in parentheses indicate the correct locations and quantities for multiple leaks in pipeline element 3.

3.2. Discussion

Leak identification signals can be obtained in field systems by considering the difference in pressure with (the signal after leak generation) and without (the signal before leak generation) leakage. However, the identified leakage signal calibration should be defined to facilitate application of the leakage detection scheme. In this study, the leak quantity was assumed to very small and the terms having $\prod_{j=1}^{n}\left(\frac{Q_{olk,k}}{2H_0}\right)_{(k=C(m,n))}$ in Eqs. (14) and (15) were assumed to be negligible. If the leak quantity is not sufficiently small that the double of the $\frac{Q_{olk,k}}{2H_0}$ terms can be neglected, the developed leak detection approach is less practically meaningful, simply because visual leak identification is feasible (e.g., in the case of rupturing of a large-diameter

Table 3
Simultaneous calibration of leaks in dual path section using predictions of single path algorithm.

Scheme	The simultaneous calibration	
Leak location	56.9 m (56.0 m)	73.7 m (72.0 m)
Leak quantity	8.5% (7.0%)	5.6% (7.0%)

The numbers in parentheses indicate the correct locations and quantities for multiple leaks in pipeline element 3.

pipeline). The nonlinear terms are combinations of multiple leakage components and multiples of $\sinh\gamma$ or $\cosh\gamma$ functions for each pipeline element, which can be neglected in the case of a small order of leakage terms.

In this study, multiple leaks were assumed to occur in a specific leakage-suspected element. Construction defects, external forces, and stresses between soil and pipeline elements are mainly responsible for leakage in field pipeline systems [38,39]. In other words, the feasibility condition for leakage generation can be confined to a specific area or elemental reach in pipeline systems. If leakage is not a local problem for systematic reasons (e.g., in the case of complete deterioration of the pipe network because of an out-of-service period), leakage detection is less meaningful from a management perspective. The scope of the multiple leakage detection using the proposed method was limited to a specific pipeline element for pipe network systems.

One distinctive difference between this study and other existing leak detection studies [9,10,12,15,16,23] of complex pipelines is that the impact of the leakages on transient signals was derived from the conventional combined pressure signal from the complex pipeline topology (loops and junctions), structures (valves and reservoirs), and abnormalities (leakages). This concentrated the calibration capability of the metaheuristic engines exclusively onto the leakages, which improved the predictability of leakages. Unlike the objective functions of most other studies, which minimize the pressure difference between the real and calibrated responses either for the time domain (such as in the transient wave reflection-based method or the transient wave-damping method) or for the frequency domain (such as the frequency response method), this study introduced the objective function to reduce the difference between the identified leakage pressure and the optimized leakage response. A similar idea for the decomposition of the leakage signal from the conventional pressure signal was reported for a simple reservoir pipeline valve system through an analytical approach for the exclusive leakage impact [29].

The proposed leakage detection algorithm does not require information on the number of unknown parameters prior to application. If the pressure data time step is sufficiently small, there is no leak number limitation for application of the single path algorithm. However, the number of leaks in the dual path section seems to be limited to three, because the optimization engine can miss the global optimum if the number of unknown parameters exceeds 8 (4 locations + 4 leak quantities). Further development of the dual path algorithm (such as implementation of stepwise calibration in multiple subsections of the dual path section) is a potential solution to the problem arising for a large number of leaks.

The calibration parameters for the single or dual path algorithms (such as T_m, t_s, and OFDPA) can be adjusted considering the pressure sensor bound, background noise, and field conditions of the pipeline. In order check the robustness of the developed method, a random noise distribution having $\pm 0.05\%$ error bounds was added to the pressure signal, considering the accuracy of commercially available pressure transducers. Both the single path algorithm and the simultaneous calibration of the dual path algorithm were used to predict multiple leaks. The optimization parameters were determined as $T_{min} = 0.25$ and $is = 2$, considering the random noise distribution in $|grad|$. Table 4 presents predictions of multiple leaks for the noise-contaminated pressure signal ($\pm 0.05\%$) of the identical pipe network in Table 1. Both the leakage locations and quantities showed accurate predictions, even though slightly less accurate predictions were obtained compared to Tables 2 and 3. Further studies need to be conducted to address the impact of noise in pipe network leak predictions. This is because the effect of noise on multiple leakage predictions can differ, depending on the locations and quantities of the leakages, their distances to the pressure sensor, and the pipe network topology between the leakages and pressure sensor. In future work, both pilot plant scaled and field pipeline tests for experimental validation of the proposed method will be required to prove the applicability of the proposed method for practical purposes.

Table 4
Leak detection results from the single path algorithm and the simultaneous calibration of the dual path algorithm using the noise-contaminated pressure signal ($\pm 0.05\%$) for five leaks in element 3 of the pipe network.

Scheme	The single path algorithm	Simultaneous dual path algorithm			
Leak location	8.96 m (8.0 m)	25.4 m (24.0 m)	40.8 m (40.0 m)	58.7 m (56.0 m)	73.4 m (72.0 m)
Leak quantity	7.8% (7.0%)	7.0% (7.0%)	8.2% (7.0%)	5.8% (7.0%)	6.4% (7.0%)

The numbers in parentheses indicate the correct locations and quantities for multiple leaks in pipeline element 3.

The impedance matrix component for the unsteady friction model can also be obtained through minor modification of the efficient MLFs for laminar and turbulent flows presented in Appendices A and B. The transfer function between the upstream and downstream nodes of the pipeline element for laminar and turbulent flow conditions can be obtained by neglecting the terms having leakage components in Eqs. (A.3), (A.4), (B.2), and (B.3). Depending on the Reynolds number variation under transient conditions, the impedance matrix components for specific elements must be switched between laminar and turbulent flow conditions. However, the steady friction considered in the example is desirable for leak detection, as a pressure response signal less than the round travel time between the two reservoirs was used.

4. Conclusion

This paper proposed a procedure to detect multiple leaks for a specific element in pipe network systems through detailed analysis of transient pressure signals.

The key aspects of the developed methodology can be summarized as follows.

An efficient multiple leak function for incorporation of the effects of multiple leaks in the impedance matrix was proposed. Identical frequency response functions were found to those given by the conventional formulation with strengths in terms of model complexity and parsimony, which also provide substantial flexibility in the leak detection scheme.

A decomposition scheme to obtain the multiple leak signal from the transient pressure response was developed. The identified leakage signals indicated the solitary impacts of individual leaks; this is useful for robust leak detection. A minor modification of the leakage decomposition procedure allowed quantitative analysis of the interference between leaks.

A sequential leak detection algorithm addressing two distinct wave travel features between the leak and pressure sensor was proposed. While the single path algorithm used the time domain reflectometry, the dual path algorithm considered all possible flow paths of the pressure response. The interaction between leaks was further considered through simultaneous calibration for all leaks identified by these two algorithms.

Several topics can be explored in future work aiming to improve the applicability of the proposed methods to field pipeline networks. First, more general pipeline structure conditions should be considered, in terms of both the modeling and prediction scheme. Many pipeline systems are equipped with various hydraulic structures such as air valves and different surge protection devices. Second, the various uncertainties in real-world systems should be properly considered in the leak detection scheme, because an unknown pipeline component or the existence of air bubbles can cause substantial disturbance and yield misleading leak predictions. Third, further flexibility in the transient wave introduction can improve the applicability of the developed algorithms, simply because abrupt surge generation is not always acceptable to pipeline management authorities in the context of water quality and secure pipeline management.

Declaration of Competing Interest

The authors declare that they have no known competing financial interests or personal relationships that could have appeared to influence the work reported in this paper.

Acknowledgement

This research was supported by South Korea Ministry of Environment as ‘Global Top Project (RE201606133)’.

Appendix A. Incorporation of efficient multiple leak formulation in impedance matrix for unsteady friction model under laminar flow conditions

The radial distribution of the velocity can be expressed by the following two-dimensional equations of motion and continuity for laminar flow conditions [40,41]:

$$\frac{1}{\rho}\frac{\partial p}{\partial x}+\frac{\partial u}{\partial t}-\nu\frac{1}{r}\frac{\partial}{\partial r}\left(r\frac{\partial u}{\partial r}\right)=0 \tag{A.1}$$

$$\rho a^2\frac{\partial u}{\partial x}+\frac{\partial P}{\partial t}=0 \tag{A.2}$$

where u,p are the velocity and pressure, respectively, as functions of time (t), axial distance (x), and radial distance (r); ν is the kinematic viscosity, and ρ is the fluid density.

The analytical expressions for the downstream complex head-discharge ratio and the upstream head-discharge and discharge-discharge ratios for incorporation of the efficient multiple leak formulation (MLF) in the impedance matrix can be approximated as follows:

$$\frac{H_D}{Q_r}=\left(cosh\Gamma(l)\frac{H_U}{Q_r}-Z_s sinh\Gamma(l)\frac{Q_U}{Q_r}\right)+(Z_s\sum_{i=1}^{m}\frac{Q_{olk,i}}{2H_o}sinh\Gamma(l-x_i)cosh\Gamma(x_i))\frac{H_U}{Q_r}-(Z_s{}^2\sum_{i=1}^{m}\frac{Q_{olk,i}}{2H_o}sinh\Gamma(l-x_i)\gamma sinh\Gamma(x_i))\frac{Q_U}{Q_r} \tag{A.3}$$

The relationship between the downstream complex discharge-discharge ratio and the upstream head-discharge and discharge-discharge ratios for incorporation of the efficient MLF into the impedance matrix can be approximated as follows:

$$\frac{Q_D}{Q_r}=\left(-\frac{\sinh\Gamma(l)}{Z_c}\frac{H_U}{Q_r}+\cosh\Gamma(l)\frac{Q_U}{Q_r}\right)-\sum_{i=1}^{m}\frac{Q_{olk,i}}{2H_o}\cosh\Gamma(l-x_i)\cosh\Gamma(x_i)\frac{H_U}{Q_r}+Z_s\sum_{i=1}^{m}\frac{Q_{olk,i}}{2H_o}\cosh\Gamma(l-x_i)\sinh\Gamma(x_i))\frac{Q_U}{Q_r} \tag{A.4}$$

where the propagation constant, $\Gamma(l)=sl/(a\sqrt{1-2J_1(\frac{iD}{2\sqrt{\frac{s}{v}}})/(iD/2\sqrt{\frac{s}{v}}J_0(iD/2\sqrt{s/v})})$, and the characteristic impedance, $Z_s=a/(gA\sqrt{1-2J_1(\frac{iD}{2\sqrt{\frac{s}{v}}})/(iD/2\sqrt{\frac{s}{v}}J_0(iD/2\sqrt{s/v})})$. Here, s is frequency, D is diameter, i is an imaginary unit, and J_0 and J_1 are the first-type Bessel functions of the zeroth and first orders, respectively.

Appendix B. Incorporation of efficient multiple leak formulation into impedance matrix for unsteady friction model under turbulent flow conditions

Considering unsteady friction due to the temporal and convective accelerations for turbulent flow conditions, Eq. (1) of the main text can be expressed as follows [42,43]:

$$\frac{1}{g}\frac{\partial V}{\partial t}+\frac{\partial H}{\partial x}+\frac{f|Q|Q}{2DA}+F_u=0 \tag{B.1}$$

where $F_u=\frac{1}{g}\left(k_1\frac{\partial V}{\partial t}+ak_2Sign(V)\left|\frac{\partial V}{\partial x}\right|\right)$; k_1 and k_2 are the unsteady friction coefficients for the temporal and convective acceleration terms, respectively; and Sign(V) = 1 if V ≥ 0, Sign (V) = -1 if V < 0.

Based on Eqs. (B.1) and (2) (of the main text), the following analytical expressions for the downstream complex head-discharge ratio and upstream head-discharge and discharge-discharge ratios for the impedance matrix can be obtained:

$$\begin{aligned}\frac{H_D}{Q_r}=&\frac{1}{Z_{c1}+Z_{c2}}\left(Z_{c1}e^{\gamma_1 l}+Z_{c2}e^{-\gamma_2 l}\right)\frac{H_U}{Q_r}+\frac{Z_{c1}Z_{c2}}{Z_{c1}+Z_{c2}}\left(-e^{\gamma_1 l}+e^{-\gamma_2 l}\right)\frac{Q_U}{Q_r}\\&-\sum_{i=1}^{m}\frac{Q_{olk}}{2H_0}\left\{\frac{Z_{c1}Z_{c2}}{(Z_{c1}+Z_{c2})^2}\left(-Z_{c1}e^{\gamma_1 l}-Z_{c2}e^{\gamma_1 x_i-\gamma_2(l-x_i)}+Z_{c1}e^{\gamma_1(l-x_i)-\gamma_2 x_i}+Z_{c2}e^{-\gamma_2 l}\right)\frac{H_U}{Q_r}+\frac{(Z_{c1}Z_{c2})^2}{(Z_{c1}+Z_{c2})^2}\left(e^{\gamma_1 l}-e^{\gamma_1 x_i-\gamma_2(l-x_i)}-e^{\gamma_1(l-x_i)-\gamma_2 x_i}+e^{-\gamma_2 l}\right)\frac{Q_U}{Q_r}\right\}\end{aligned} \tag{B.2}$$

The relationship between the downstream complex discharge-discharge ratio and the upstream head-discharge and discharge-discharge ratios in the impedance matrix can be expressed as follows:

$$\begin{aligned}\frac{Q_D}{Q_r}=&\frac{1}{Z_{c1}+Z_{c2}}\left(e^{\gamma_1 l}+e^{-\gamma_2 l}\right)\frac{H_U}{Q_r}+\frac{1}{Z_{c1}+Z_{c2}}\left(Z_{c2}e^{\gamma_1 l}+Z_{c1}e^{-\gamma_2 l}\right)\frac{Q_U}{Q_r}\\&-\sum_{i=1}^{m}\frac{Q_{olk}}{2H_0}\left\{\frac{1}{(Z_{c1}+Z_{c2})^2}\left(Z_{c1}Z_{c2}e^{\gamma_1 l}+Z_{c2}{}^2e^{\gamma_1 x_i-\gamma_2(l-x_i)}+Z_{c1}{}^2e^{\gamma_1(l-x_i)-\gamma_2 x_i}+Z_{c1}Z_{c2}e^{-\gamma_2 l}\right)\right.\\&\left.+\frac{Z_{c1}Z_{c2}}{(Z_{c1}+Z_{c2})^2}\left(-Z_{c2}e^{\gamma_1 l}+e^{\gamma_1 x_i-\gamma_2(l-x_i)}-e^{\gamma_1(l-x_i)-\gamma_2 x_i}+Z_{c3}e^{-\gamma_2 l}\right)\frac{Q_U}{Q_r}\right\}\end{aligned} \tag{B.3}$$

where the propagation constants γ_1 and γ_2 can be defined as $\gamma_{1,2}=(\mp mCs+\sqrt{(mCs)^2+4(s^2CL+RCs)})/2$; $m=(ak_2)/(2gA)$; the capacitance, $C=(gA)/a^2$; the inertance, $L=(1+k_1)/(gA)$; the resistance per unit length, $R=(f\overline{Q})/(gDA^2)$ for turbulent flow; and the characteristic impedances are $Z_{c1},Z_{c2}=\frac{\gamma_1}{Cs},\frac{\gamma_2}{Cs}$.

References

[1] M. Ferrante, B. Brunone, S. Meniconi, B.W. Karney, C. Massari, Leak size, detectability and test conditions in pressurized pipe systems, Water Resour. Manage. 28 (13) (2014) 4583–4598.
[2] A. Haghighi, H.M. Ramos, Detection of leakage freshwater and friction factor calibration in drinking networks using central force optimization, Water Resour. Manage. 26 (8) (2012) 2347–2363.
[3] M.R. Karim, M. Abbaszadegan, M. Lechevallier, Potential for pathogen intrusion during pressure transients, J. Amer. Water Works Assoc. 95 (5) (2003) 134–146.
[4] J.A. Liggett, L.-C. Chen, L, Inverse transient analysis in pipe networks, J. Hydraulic Eng. 120 (8) (1994) 934–955.
[5] J.P. Vítkovský, A.R. Simpson, M.F. Lambert, Leak detection and calibration using transient and genetic algorithms, J. Water Resour. Plann. Manage. 126 (4) (2000) 262–265.
[6] W. Mpesha, S.L. Gassman, M.H. Chaudhry, Leak detection in pipes by frequency response method, J. Hydraulic Eng. 127 (2) (2001) 134–147.

[7] P.J. Lee, J.P. Vítkovský, M.F. Lambert, A.R. Simpson, J.A. Liggett, Leak location using in pattern of the frequency response diagram in pipelines: a numerical study, J. Sound Vib. 284 (3) (2005) 1051–1073.
[8] A.F. Colomb, P.J. Lee, B.W. Karney, A selective literature review of transient-based leak detection methods, J. Hydro-Environ. Res. 2 (2009) 212–227.
[9] D. Covas, H. Ramos, (2010) Case studies of leak detection and location in water pipe systems by inverse transient analysis, J. Water Resour. Plann. Manage. 136 (2) (2010) 248–257.
[10] H.-F. Duan, P.J. Lee, M.S. Ghidaoui, Y.-K. Tung, Leak detection in complex series pipelines by using frequency response method, J. Hydraul. Res. 49 (2) (2011) 213–221.
[11] H.-F. Duan, P.J. Lee, M.S. Ghidaoui, Y.-K. Tung, System response function based leak detection in viscoelastic pipelines, J. Hydraulic Eng. 138 (2) (2011) 143–153.
[12] A.C. Zecchin, L.B. White, M.F. Lambert, A.R. Simpson, Parameter identification of fluid line networks by frequency domain maximum likelihood estimation, Mech. Syst. Signal Process. 37 (1) (2013) 370–387.
[13] S. Meniconi, H.F. Duan, P.J. Lee, B. Brunone, M.S. Ghidaoui, M. Ferrante, Experimental investigation of coupled frequency and time-domain transient test-based techniques for partial blockage detection in pipelines, J. Hydraul. Eng. 139 (10) (2013) 1033–1040, https://doi.org/10.1061/(ASCE)HY.1943-7900.0000768.
[14] H.-F. Duan, P.J. Lee, M.S. Ghidaoui, J. Tuck, Transient wave-blockage interaction and extended blockage detection in elastic water pipelines, J. Fluids Struct. 46 (2014) 2–16.
[15] S.-H. Kim, Impedance method for abnormality detection of a branched pipeline system, Water Resour. Manage. 30 (3) (2016) 1101–1115.
[16] H.-F. Duan, Transient frequency response based leak detection in water supply pipeline systems with branched and looped junctions, J. Hydroinf. 19 (1) (2017) 17–30.
[17] S.T.N. Nguyen, J. Gong, M.F. Lambert, A.C. Zecchine, A.R. Simpson, Least square deconvolution for leak detection with a pseudo random binary sequence excitation, Mech. Syst. Signal Process. 99 (2018) 846–858.
[18] Bruno Brunone, Marco Ferrante, Silvia Meniconi, Portable pressure wave-maker for leak detection and pipe system characterization, J. Am. Water Works Assoc. 100 (4) (2008) 108–116, https://doi.org/10.1002/j.1551-8833.2008.tb09607.x.
[19] P.J. Lee, J.P. Vítkovský, M.F. Lambert, A.R. Simpson, Valve design for extracting response functions from hydraulic systems using peudorandom binary signal, J. Hydraulic Eng. 136 (4) (2008) 858–864.
[20] J. Gong, M.F. Lambert, S.T.N. Nguyen, A.R. Simpson, Detecting thinner-walled pipe sections using a spark transient pressure wave generator, J. Hydraulic Eng. 144 (2) (2018) 06017027.
[21] S. Meniconi, B. Brunone, M. Ferrante, In-line pipe device checking by shot-period analysis of transient tests, J. Hydraulic Eng. 137 (7) (2011) 713–722.
[22] A.M. Satter, M.H. Chaudhry, A.A. Kassem, Partial blockage detection in pipelines by frequency response method, J. Hydraulic Eng. 134 (1) (2008) 76–89.
[23] H.-F. Duan, P.J. Lee, Transient-based frequency domain method for dead-end side branch detection in reservoir pipeline valve systems, J. Hydraulic Eng. 142 (2) (2015) 04015042.
[24] Jinzhe Gong, Mark L Stephens, Nicole S Arbon, Aaron C Zecchin, Martin F Lambert, Angus R Simpson, On-site non-invasive condition assessment for cement mortar–lined metallic pipelines by time-domain fluid transient analysis, Struct. Health Monitor. 14 (5) (2015) 426–438, https://doi.org/10.1177/1475921715591875.
[25] B. Brunone, Transient test-based technique for leak detection in outfall pipes, J. Water Resour. Plann. Manage. 125 (5) (1999) 302–306.
[26] S.-H. Kim, A. Zecchine, R.W. Choi, Diagnosis of a pipeline system for transient flow in low Reynolds number with impedance method, J. Hydraulic Eng. 140 (12) (2014), https://doi.org/10.1061/(ASCE)HY.1943-7900.0000945.
[27] P.J. Lee, H.-F. Duan, M.S. Ghidaoui, B. Karney, Frequency domain analysis of pipe fluid transient behavior, J. Hydraulic Res. 51 (6) (2013) 609–622.
[28] M.H. Ranginkaman, A. Haghighi, P.J. Lee, Frequency domain modelling of pipe transient flow with the virtual valves method to reduce linearization errors, Mech. Syst. Signal Process. 131 (2019) 486–504.
[29] S.-H. Kim, Development of multiple leakage detection method for a reservoir pipeline valve system, Water Resour. Manage. 32 (6) (2018) 2099–2112.
[30] X. Wang, M.S. Ghidaoui, Identification of multiple leaks in pipeline: linearrized model, maximum likelihood, and super-resolution localization, Mech. Syst. Signal Process. 107 (2018) 529–548.
[31] X. Wang, M.S. Ghidaoui, Identification of multiple leaks in pipeline II: iterative beamforming and leak number estimation, Mech. Syst. Signal Process. 119 (2019) 346–362.
[32] M. Ferrante, B. Brunone, S. Meniconi, B.W. Karney, C. Massari, Leak size, detectability and test conditions in pressurized pipe system, Water Resour. Manage. 28 (13) (2014) 4583–4598.
[33] E.B. Wylie, V.L. Streeter, Fluid transient in systems. Prentice Hall, Inc., Englewood Cliffs, N J. 1993
[34] M.H. Chaudhry, Applied Hydraulic Transient, third ed., Springer, 2014.
[35] S.-H. Kim, Impedance matrix method for transient analysis of complicated pipe networks, J. Hydraulic Res. 45 (6) (2007) 818–828.
[36] D.E. Goldberg, Genetic Algorithms in Search, Optimization and Machine Learning, Addison-Wesley Publishing Co. Inc, Reading, MA, 1989.
[37] J. Kennedy, R. Eberhart, Particle Swarm Optimization. Proceedings of IEEE International Conference on Neural Networks. IV. 1942–1948. 1995.
[38] H. Kishaway, H. Gabbar, Review of pipeline integrity management practices, Int. J. Pressure Vessels Piping 87 (7) (2010) 373–380.
[39] H. Wang, I. Duncan, Likelihood, causes, and consequences of focused leakage and rupture of U.S. natural gas transmission pipelines, J. Loss Prevent. Process Indus. 30 (2014) 177–187.
[40] L. Suo, E.B. Wylie, Impulse response method for frequency-dependent pipeline transients, J. Fluids Eng. Trans. ASME 111 (4) (1989) 478–483.
[41] W. Zielke, Frequency-dependent friction in transient pipe flow, J. Basic Eng. ASME 90 (1) (1968) 109–115.
[42] B. Brunone, U.M. Golia, M. Greco, Some remarks on the momentum equations for fast transients. Hydraulic transients with column separation 9th and last round table of IAHR Group, IAHR, Valencia, Spain, 201-209. 1991.
[43] H. Ramos, D. Covas, A. Borga, D. Loureiro, Surge damping in pipe systems: modeling and experiments, J. Hydraulic Res. 42 (4) (2004) 413–425.